Received: 30 August 2023 | Revised: 21 May 2024 | Accepted: 24 May 2024

DOI: 10.1002/env.2869

RESEARCH ARTICLE

WILEY

Achieving spatial balance in environmental surveys under constant inclusion probabilities or inclusion density functions

Rosa M. Di Biase[1,2] | **Marzia Marcheselli**[1,2] | **Caterina Pisani**[1,2]

[1]Department of Economics and Statistics, University of Siena, Siena, Italy

[2]NBFC, National Biodiversity Future Center, Palermo, Italy

Correspondence
Rosa M. Di Biase, Department of Economics and Statistics, University of Siena, Siena, Italy.
Email: rosa.dibiase@unisi.it

Funding information
National Recovery and Resilience Plan (NRRP); European Union—NextGenerationEU, Grant/Award Number: CN_00000033

Abstract

In environmental and ecological surveys, well spread samples can be easily obtained via widely adopted tessellation schemes, which yield equal first-order inclusion probabilities in the case of finite populations of areas or constant inclusion density functions in the case of continuous populations. In the literature, many alternative schemes that are explicitly tailored to select well spread samples have been proposed, but owing to their complexity, their use should be preferred only if they allow us to achieve a valuable gain in precision with respect to the tessellation schemes. Therefore, by means of an extensive simulation study, the performances of tessellation schemes and several specifically tailored schemes are compared under constant first-order inclusion probabilities or constant inclusion density functions.

KEYWORDS

continuous populations, efficiency, finite populations of areas, tessellation sampling schemes, total estimation, well spread samples

1 | INTRODUCTION

Assessing and monitoring natural resources and biodiversity is a pressing issue in environmental and ecological studies, and for this purpose, the totals of interest attributes and the suitable functions of totals commonly constitute relevant parameters to be estimated. For example, ecologists and foresters may be interested in the coverage of habitat types, species richness and species abundance vectors, which can be suitably expressed as totals, and in quantifying diversity indices, which invariably are functions of the species abundance vector.

Design-based inference has been widely adopted for estimating totals of attributes in environmental spatial populations (e.g., De Vries, 1986; Thompson, 2002; Gregoire and Valentine, 2008; De Gruijter et al., 2010), and in this framework, spatial populations are constituted by fixed sets of locations in a study region with fixed values of the survey variable attached to each location. Populations can be distinguished as continuous populations and finite populations of areas or units, and totals can be expressed as integrals or summands, respectively.

In the case of populations of units, the list, and obviously the location, of the units (e.g., trees in a forest stand, shrubs in a natural reserve) is rarely available and involves prohibitive efforts, especially over large areas. Accordingly, populations of units are commonly sampled using points (eventually identifying plots or transects) selected in the study region in such a way that the total can be expressed as the integral of a suitable function defined on the continuum of points. In this

case, total estimation can be reinterpreted as the estimation of the total of a continuous population (see, e.g., Gregoire & Valentine, 2007; Mandallaz, 2007; Stevens & Urquhart, 2000). Therefore, in this article, only the total estimation of continuous and finite populations of areas is considered.

To increase the precision of total estimators, the sampling of locations that are "well spread" throughout the study region plays an essential role in environmental surveys owing to the two major characteristics of spatial populations: i) the presence of positive spatial autocorrelation, that is, the values of the survey variable in neighboring locations tend to be similar, as they interact with one another and are influenced by the same factors (Stevens & Olsen, 2004); and ii) the presence of spatial heterogeneity of the survey variable between different portions of the study region. Therefore, the selection of neighboring locations should be avoided, and no portion of the study region should be over- or underrepresented in the sample. Grafström and Lundström (2013) make heuristic arguments regarding how spatially balanced samples can increase the precision of the Horvitz–Thompson (HT) estimator in the framework of finite populations. A more rigorous justification for the need for spatially balanced samples in the presence of positive spatial autocorrelation and auxiliary information is given by Grafström and Tillé (2013).

Following Grafström et al. (2012) and Grafström and Matei (2018) we refer to a well spread sample as a spatially balanced sample. well spread samples can be straightforwardly obtained using sampling schemes that are widely adopted in environmental and ecological surveys, commonly implemented by suitably partitioning the study region or by superimposing a regular grid on it, and therefore referred to as tessellation sampling schemes (e.g., Tomppo et al., 2010 for applications in forest inventories). In particular, for continuous populations, well spread samples are achieved adopting tessellation stratified sampling or systematic grid sampling, while for finite populations of areas, they are achieved using one-per-stratum stratified sampling or systematic sampling.

The achievement of well spread samples has long been the main target, and many schemes have been explicitly tailored to this purpose (for a review, see, e.g., Benedetti et al., 2017; Kermorvant et al., 2019). The main goal of this paper is to compare the performances, in terms of the precision of the estimates, of the tessellation schemes and of several specifically tailored schemes. Indeed, owing to their complexity, specifically tailored schemes should be implemented only if they guarantee a valuable gain in precision with respect to tessellation schemes. We considered only schemes implemented in R open packages, which make their use possible for field scientists and practitioners. Moreover, as tessellation schemes generally yield equal first-order inclusion probabilities or constant inclusion density functions, more complex schemes will also be implemented with constant inclusion probabilities or inclusion density functions, even though some of them can perform well when unequal probabilities are used. However, in environmental surveys, the selected sample is often adopted to estimate the total of several variables of interest. Therefore, the auxiliary variable considered for selecting unequal probability samples may be different for each total of interest in such a way that the choice may be problematic. On the other hand, under tessellation schemes, auxiliary variables could be alternatively adopted at the estimation level.

In this paper, we perform a comparison of sampling schemes without considering any auxiliary information. In Section 2, some preliminaries are given, and in Section 3, definitions of spatial balance and spatial balance measures are discussed. In Section 4, schemes explicitly tailored for achieving spatial balance and the tessellation sampling schemes are briefly described. Section 5 is devoted to an extensive simulation study, and concluding remarks are given in Section 6.

2 | PRELIMINARIES AND NOTATION

2.1 | Continuous populations

Continuous populations are continuous sets of locations with a surface giving the values of the density of a survey variable (e.g., density of the aboveground biomass, density of soil or water pollutants) at each location. Let y be a Borelian and bounded function on the study region $\mathcal{A}$, where $y(\mathbf{p})$ is the value of the density at the location $\mathbf{p} \in \mathcal{A}$, and the population total is given by

$$T = \int_{\mathcal{A}} y(\mathbf{p})\lambda(d\mathbf{p}), \tag{1}$$

where λ is the Lebesgue measure in R^2.

Let $\{\mathbf{P}_1, \ldots, \mathbf{P}_n\}$ be a sample of locations selected according to a probabilistic sampling design giving rise to the inclusion density function $\pi(\mathbf{p})$ and pairwise inclusion density function $\pi(\mathbf{p}, \mathbf{q})$, for any $\mathbf{p}, \mathbf{q} \in \mathcal{A}$. If $\pi(\mathbf{p}) > 0$ for any $\mathbf{p} \in \mathcal{A}$,

an unbiased estimator of T is the continuous analogue of the HT estimator (Cordy, 1993)

$$\widehat{T} = \sum_{j \in S} \frac{y(\mathbf{P}_j)}{\pi(\mathbf{P}_j)}, \tag{2}$$

where S is the set of indices that identify the sampled locations.

Moreover, if $\int_{\mathcal{A}} 1/\pi(\mathbf{p})\lambda(d\mathbf{p}) < \infty$, the variance is

$$\mathrm{V}(\widehat{T}) = \int_{\mathcal{A}} \frac{y^2(\mathbf{p})}{\pi(\mathbf{p})}\lambda(d\mathbf{p}) + \int_{\mathcal{A}^2} \left\{ \frac{\pi(\mathbf{p},\mathbf{q})}{\pi(\mathbf{p})\pi(\mathbf{q})} - 1 \right\} y(\mathbf{p})y(\mathbf{q})\lambda(d\mathbf{p})\lambda(d\mathbf{q}),$$

which is unbiasedly estimated if $\pi(\mathbf{p},\mathbf{q})$ is strictly positive for any $\mathbf{p},\mathbf{q} \in \mathcal{A}$ by using the continuous analogue of the HT variance estimator or, if the sample size is fixed, of the Sen–Yates–Grundy estimator (Cordy, 1993; Stevens & Olsen, 2003). When a scheme for selecting spatially balanced samples is considered, thus avoiding the selection of neighboring locations, the pairwise inclusion density function is not strictly positive, and conservative estimators can be adopted (Stevens & Olsen, 2003).

2.2 | Finite populations of areas

Finite populations of areas are obtained by partitioning the study region into regular polygons (such as satellite pixels) or irregularly shaped areal units (such as administrative districts), and the survey variable is the total amount of an attribute (e.g., species abundance, aboveground biomass, growing stock volume, mineral contaminants, soil or water pollutants) within each area.

Formally, let U be the population of N areas, indexed by the N first integers, and let $\mathcal{A}_1, \ldots, \mathcal{A}_N$ be the N areas. In this framework, two cases are distinguished: a fixed density function of an attribute of interest is defined for any location of the study region, or a finite population of units is located in the study region, equipped with a fixed value of an attribute of interest. Let y_j denote the total amount of the attribute of interest in the jth area. In particular, in the first case, y_j is obtained as the integral of the density function on $\mathcal{A}_j$, while in the second case, it is the sum of the attribute values for the units located in the jth area. The population total is given by

$$T = \sum_{j \in U} y_j. \tag{3}$$

Notably, finite populations of areas can be regarded as with-list finite populations of units, where each area is a unit whose location is given by the centroid of the area.

Let $S \subset U$ be a probabilistic sample of size n, and π_j is the first-order inclusion probability of the jth area ($j = 1, \ldots, N$), and the HT estimator of the total

$$\widehat{T} = \sum_{j \in S} \frac{y_j}{\pi_j} \tag{4}$$

with variance

$$\mathrm{V}(\widehat{T}) = \sum_{j \in U} \left(\frac{1-\pi_j}{\pi_j} \right) y_j^2 + 2 \sum_{j>h \in U} \left(\frac{\pi_{jh}}{\pi_j \pi_h} - 1 \right) y_j y_h,$$

where π_{jh} is the second-order inclusion probability of areas j and h, $j \neq h = 1, \ldots, N$.

If all the second-order inclusion probabilities are strictly positive, $\mathrm{V}(\widehat{T})$ can be unbiasedly estimated by using the HT variance estimator or, if the sample size is fixed, the Sen–Yates–Grundy estimator. When some second-order inclusion probabilities are equal to zero, such as when considering designs that avoid the selection of contiguous areas, conservative estimators can be adopted (see e.g., Wolter, 2007).

3 | MEASURING SPATIAL BALANCE

According to some authors (Benedetti et al., 2017; Grafström & Lundström, 2013; Grafström et al., 2012; Grafström & Schelin, 2014), a sample is said to be well spread or spatially balanced if the number of selected units is close to what is expected on average in every part of the study region. As first suggested by Stevens and Olsen (2004), the spatial balance of a realized sample can be quantified by using Voronoi polytopes. In particular, in the case of continuous populations, the Voronoi polygon $\mathcal{V}_j$ associated with the jth sampled location $\mathbf{p}_j$ ($j \in S$) is the set of all the locations with smaller distances to $\mathbf{p}_j$ with respect to any other sampled location and

$$v_j = \int_{\mathcal{V}_j} \pi(\mathbf{p})\lambda(d\mathbf{p})$$

represents the expected number of locations selected into the polygon under the considered sampling scheme. Analogously, in the case of finite populations of areas whose locations are identified via the area centroid, the Voronoi polygon $\mathcal{V}_j$ is the set of all the areas whose centroids are closer to the centroid of the jth sampled area than to those of all the other sampled areas and

$$v_j = \sum_{i \in \mathcal{V}_j} \pi_i$$

is the expected number of areas in the polygon selected under the implemented scheme.

Thus, more formally (see, e.g., Grafström & Matei, 2018; Grafström & Lundström, 2013), a sample is said to be spatially balanced if each v_j is equal to (or close to) 1. When addressing continuous populations, if the sampling scheme ensures constant inclusion density functions, a sample is spatially balanced if all the polygons are approximately equal in size. Similarly, if equal first-order inclusion probability designs are considered for sampling populations of areas, a sample is spatially balanced if each polygon is formed by approximately the same number of areas.

To quantify the degree of spatial balance of a selected sample, Stevens and Olsen (2004) introduced the following straightforward measure

$$B = \frac{1}{n}\sum_{j \in S}(v_j - 1)^2, \tag{5}$$

which is probably the most widely adopted (e.g., Grafström & Lundström, 2013; Grafström, Zhao, et al., 2017). Notably, lower values indicate higher degrees of spatial balance, and $B = 0$ when the sample is spatially balanced.

Recently, referring to finite populations, Tillé et al. (2018) noted that the feasible range of B depends on the spatial pattern of the population and hence differs among different populations. Therefore, B can be successfully employed to compare the level of spatial balance of different samples from the same population. Tillé et al. (2018) proposed an alternative approach for measuring the spatial balance of a realized sample based on a standardized version of the Moran index, with spatial weights taking into account both the distance among units and their first-order inclusion probabilities. Alternatively, Jauslin and Tillé (2020) suggested the use of different weight specifications.

All these measures allow us to quantify the degree of spatial balance of an already selected sample, and to assess whether a given sampling scheme succeeds in producing spatially balanced samples, the expected value of those measures must be computed by means of a simulation.

On the other hand, Fattorini, Marcheselli, Pisani, and Pratelli (2018) and Fattorini, Marcheselli, and Pratelli (2018) proposed a definition of asymptotically spatially balanced sampling schemes in the framework of the infill paradigm (Cressie, 1993). In the case of continuous populations, the population is held fixed such that T, as defined in (1), is also fixed. Then, for any natural number k, a fixed-size design is considered to select a sample of increasing n_k locations with $n_k \to \infty$ as k increases. Let $Z_k(\mathbf{p}, \delta)$ be the number of sampled locations in the closed disc of radius δ centered at $\mathbf{p}$. A sampling scheme is asymptotically spatially balanced if, for any $\mathbf{p} \in \mathcal{A}$ and any $\varepsilon > 0$, there exist $C > 0$ and an integer k_0 such that

$$\Pr\{Z_k(\mathbf{p}, C/\sqrt{n_k}) = 0\} < \varepsilon \qquad \forall \ \ k > k_0. \tag{6}$$

Then, a sampling scheme is defined to be asymptotically spatially balanced if, as the sample size increases, the scheme is able to evenly spread the sample in such a way that any location of the study region is likely to have neighboring locations sampled. Additionally, in the case of finite populations of areas, T, which is defined in (3), is fixed. In this case, for any natural number k, the study region is partitioned into an increasing number N_k of areas where as k increases, $N_k \to \infty$. Then, a sequence of fixed-size designs is considered to select samples of $n_k < N_k$ with $n_k \to \infty$ and a definition of an asymptotically spatially balanced sampling scheme analogous to (6) can be given.

The definition of asymptotic spatial balance refers to the sampling scheme, unlike the previous definitions that apply to a realized sample, and thus, in principle, allows us to determine if a sampling scheme is able to select asymptotically spatially balanced samples before sample selection. In particular, tessellation sampling schemes have been proven to be asymptotically spatially balanced (Fattorini, Marcheselli, Pisani, & Pratelli, 2018; Fattorini, Marcheselli, & Pratelli, 2018).

4 | SAMPLING SCHEMES EXPLICITLY TAILORED FOR SPATIAL BALANCE

Numerous studies are devoted to constructing spatially balanced sampling schemes for continuous and finite populations of units. This section does not constitute an exhaustive and complete review of these sampling schemes, as we focused on those implemented in R open packages, which make their use possible for field scientists and practitioners.

Generalized Random Tessellation Stratified (GRTS) sampling (Stevens & Olsen, 2004) is likely one of the most popular scheme. GRTS sampling recursively partitions a grid superimposed on the study region into quadrants and hierarchically attaches an ordered spatial address to each quadrant. The spatial addresses are reorganized and mapped into a one-dimensional space, preserving proximity relationships as much as possible, and sampled via a systematic design. GRTS sampling can be adopted for continuous and finite populations and allows the selection of samples with prescribed first-order inclusion densities or probabilities, respectively.

Another spatially balanced sampling scheme for continuous and finite populations is Balanced Acceptance Sampling (BAS) (Robertson et al., 2013; Robertson et al., 2017), which utilizes a quasirandom number sequence called the random-start Halton sequence, to spread the sample across multiple dimensions. Target inclusion probabilities or inclusion density functions can generally be achieved under BAS, which is suitable for continuous populations but can be inefficient for certain finite populations (Robertson et al., 2018). Moreover, Robertson et al. (2018) proposed a sampling scheme called Halton Iterative Partitioning (HIP), an alternative to BAS, which shares desirable properties without having drawbacks in achieving target inclusion probabilities when sampling finite populations. This design uses structural properties of the Halton sequence, rather than points from the sequence, to draw the sample. HIP can be applied to finite and continuous populations and with equal or unequal inclusion probabilities and inclusion density functions.

In the framework of finite populations, Grafström (2012) suggested Spatially Correlated Poisson Sampling (SCPS), a variation of Correlated Poisson Sampling (CPS), which was introduced by Bondesson and Thorburn (2008). CPS is a list sequential scheme that allows for the achievement of prescribed first-order inclusion probabilities. In particular, each population unit is considered according to its position in the list, its inclusion in the sample is randomly decided, and the inclusion probabilities for the remaining units are updated by using weights. Under SPCS, weights take into account the distances between units and are chosen to create a strong negative correlation between the sample inclusion indicators of nearby units, to preclude units close to the previously sampled units from being selected.

The introduction of a distance between two population units also allows Grafström et al. (2012) to incorporate the spatial component into the Pivotal Method (PM) by Deville and Tillé (1998), producing the Local Pivotal Method (LPM). PM is a sequential sampling scheme that allows the achievement of prescribed first-order inclusion probabilities, where at each step, the inclusion probabilities are updated for two units in such a way that the sampling outcome is decided for at least one of the two units. As in SCPS, the main idea of LPM is to create a strong negative correlation between the sample inclusion indicators of units that are close in distance. With the LPM, at each step, the inclusion probabilities of two nearby units are updated so that either one unit enters the sample or one unit is excluded from the sample. As only nearby units compete with each other for inclusion in the sample, LPM tends to produce locally spatially balanced samples. Notably, the LPM has recently been adopted for selecting well spread samples in the framework of continuous populations using some form of double sampling (Grafström, Schnell, et al., 2017; Grafström & Matei, 2018).

When addressing finite populations, Grafström and Tillé (2013) propose the use of a sampling scheme with prescribed first-order inclusion probabilities and that can achieve a double property of balancing: the sample is both spatially balanced and balanced on several auxiliary variables, that is, well spread and such that the HT total estimator is almost equal to the population totals for these variables. This scheme, which is referred to as Doubly Balanced Spatial Sampling

(DBSS), is obtained by combining a generalization of LPM and the cube method by Deville and Tillé (2004). The basic idea of DBSS is to repeatedly apply the "flight phase" of the cube method to a cluster of nearby units, updating their first-order inclusion probabilities while respecting the balancing conditions. For each cluster, the sampling outcome is determined for at least one unit, which is either selected or excluded from the sample.

More recently, Jauslin and Tillé (2020) proposed a sampling scheme based on the definition of a spatial structure via stratification, allowing the achievement of prescribed first-order inclusion probabilities. The sampling scheme, denoted as Weakly Associated Vector Sampling, is implemented in the R package "WaveSampling" (Jauslin & Tillé, 2022). However, its use can be precluded if the population size is greater that 500, which is quite common in large-scale surveys. In this case, the time needed for sample selection can be unfeasible.

Notably, under spatially balanced sampling, second-order inclusion probabilities may be zero or very close to zero for units that are close in distance, thus precluding unbiasedly estimating the variance of the HT estimator. Thus, to estimate precision, conservative estimators (e.g., Stevens & Olsen, 2004) or ad hoc estimators (e.g., Fattorini, 2006; Grafström & Schelin, 2014; Grafström & Tillé, 2013; Stevens & Olsen, 2003) must be adopted.

5 | TESSELLATION SAMPLING SCHEMES

When a continuous population is considered, the most straightforward schemes for obtaining a well-spread sample are tessellation stratified sampling (TSS) and systematic grid sampling (SGS), both of which have long been used in the statistical literature (see e.g., Stevens, 1997). Under TSS, the study region is partitioned into n spatial subsets of equal extent, and a location is randomly and independently selected in each subset. Alternatively, TSS can be performed by covering the study region with a grid of regular polygons of equal size (Barabesi et al., 2012) and then randomly and independently selecting a location in each polygon.

SGS is implemented by partitioning the study region into n regular polygons of equal extent or, more commonly, by superimposing a grid of regular polygons on the study region (Barabesi et al., 2012). In particular, under SGS, a point is randomly selected in one polygon and systematically repeated in the polygons. Both TSS and SGS are largely applied in forest inventories, especially at large scales (such as national inventories), where they are commonly performed using grids of regular polygons of equal size (e.g., quadrats in the Italian National Forest Inventory and hexagons in the US Forest Inventory).

The theoretical properties of both designs were investigated by Barabesi et al. (2012). In particular, the authors proved that under some smoothness conditions on y, TSS gives rise to an unbiased "superefficient" estimator of T with respect to that obtained under uniform random sampling (URS), which consists of randomly and independently selecting the locations on the study region and thus produces equal inclusion density functions. In particular, the variance of $\widehat{T}$ under TSS is of order $n^{-\gamma}$, where $\gamma \in (1, 2]$. However, under URS, the variance of $\widehat{T}$ is of order n^{-1}. Additionally, SGS may allow

FIGURE 1 Estimated land use map in the square region located in South Tuscany: the integers from 1 to 5 identify forestland, cropland, grassland, wetland and settlements, respectively.

TABLE 1 Mean values of *B*, percentage ERSE and efficiencies of the HT estimator of forestland, cropland and grassland coverage with respect to TSS.

			Forest land		Cropland		Grassland	
Scheme	***n***	$\overline{B}$	**ERSE (%)**	**Eff**	**ERSE (%)**	**Eff**	**ERSE (%)**	**Eff**
TSS	144	0.0639	4.14	1	10.97	1	43.11	1
	361	0.0629	2.26	1	5.80	1	24.75	1
	900	0.0622	1.17	1	3.05	1	11.81	1
SGS	144	0.0279	3.09	0.75	8.10	0.74	42.84	0.99
	361	0.0176	1.40	0.62	3.54	0.61	20.79	0.84
	900	0.0112	1.03	0.88	2.61	0.86	7.65	0.65
GRTS	144	0.1088	4.30	1.04	11.28	1.03	45.66	1.06
	361	0.1066	2.47	1.10	6.41	1.11	26.09	1.05
	900	0.1036	1.39	1.19	3.58	1.18	14.62	1.24
BAS	144	0.0522	3.76	0.91	9.49	0.87	47.64	1.11
	361	0.0634	2.04	0.90	5.76	0.99	21.93	0.89
	900	0.0563	1.07	0.91	3.03	0.99	11.31	0.96
HIP	144	0.0525	3.77	0.91	9.57	0.87	47.52	1.10
	361	0.0634	2.03	0.90	5.74	0.99	21.48	0.87
	900	0.0565	1.05	0.90	2.98	0.98	11.20	0.95

TABLE 2 Mean values of *B*, percentage ERSE and efficiencies of the HT estimator of wetland and settlements coverage with respect to TSS.

			Wetland		Settlements	
Scheme	***n***	$\overline{B}$	**ERSE (%)**	**Eff**	**ERSE (%)**	**Eff**
TSS	144	0.0639	112.71	1	89.77	1
	361	0.0629	63.06	1	44.96	1
	900	0.0622	36.00	1	22.64	1
SGS	144	0.0279	86.82	0.77	94.57	1.06
	361	0.0176	41.88	0.66	29.46	0.66
	900	0.0112	19.76	0.55	16.59	0.73
GRTS	144	0.1088	117.65	1.04	89.77	1
	361	0.1066	64.71	1.03	51.16	1.14
	900	0.1036	36.00	1.00	27.91	1.23
BAS	144	0.0522	139.53	1.24	88.37	0.99
	361	0.0634	73.65	1.17	44.96	1
	900	0.0563	31.29	0.87	22.33	0.98
HIP	144	0.0525	137.88	1.22	88.06	0.98
	361	0.0634	74.35	1.18	45.27	1.01
	900	0.0565	31.29	0.87	22.33	0.99

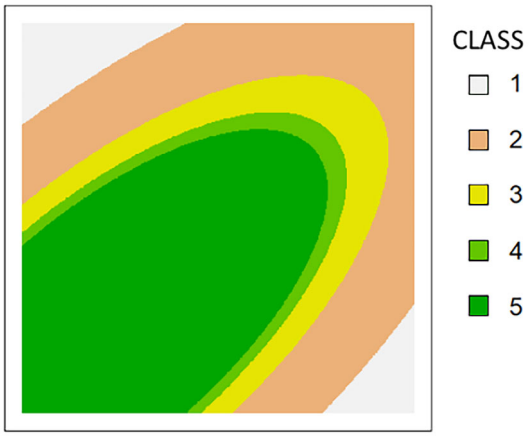

FIGURE 2 Artificial land use map: categories indexed by integers from 1 to 5.

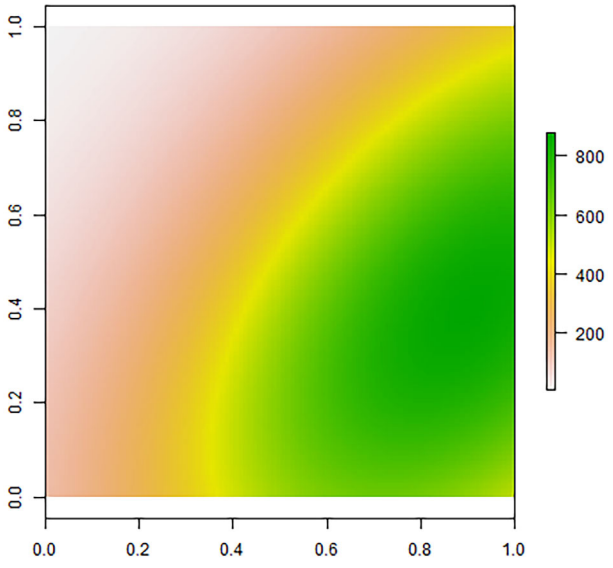

FIGURE 3 Artificial continuous population.

for a superefficient estimation, even though its variance tends to be extremely elevated if y exhibits particular periodicities or regularities.

Under the previously introduced infill asymptotic framework, TSS and SGS are asymptotically spatially balanced according to the definition by Fattorini, Marcheselli, Pisani, and Pratelli (2018) since, when the sample size increases, the probability that any location of the region has no sampled locations in a suitable neighborhood becomes definitively small. Moreover, TSS and SGS ensure that the continuous counterpart of the HT estimator is design-based consistent (Fattorini et al., 2020). Under mild conditions, both TSS and SGS also guarantee the design-based consistency of the map obtained by estimating $y(\mathbf{p})$ using the inverse weighting interpolator (Fattorini, Marcheselli, Pisani, & Pratelli, 2018).

In the framework of finite populations of areas, spatial balance can be readily obtained by using one-per-stratum stratified sampling (OPSS) and systematic sampling (SYS), both of which have a long history in the statistical literature (e.g., Breidt, 1995). Under OPSS, the areas are grouped into n strata of approximately the same number of contiguous areas, and one area is randomly selected within each stratum. If the areas are regular polygons partitioning the study region, SYS can also be performed by grouping them into n equally shaped blocks, randomly selecting a polygon in a stratum and systematically repeating the selection in the remaining strata. Regarding the precision of the HT estimator, the relative efficiency of OPSS with respect to simple random sampling without replacement (SRSWOR), which is considered a benchmark, can be straightforwardly obtained for sufficiently large strata sizes (see e.g., Hedayat & Sinha, 1991, p. 267). It

TABLE 3 Mean values of B, percentage ERSE and efficiencies of the HT estimator of the coverage of the first three categories with respect to TSS.

			Category 1		Category 2		Category 3	
Scheme	***n***	$\overline{B}$	**ERSE (%)**	**Eff**	**ERSE (%)**	**Eff**	**ERSE (%)**	**Eff**
TSS	144	0.0641	11.07	1	5.44	1	13.28	1
	361	0.0630	5.55	1	2.79	1	6.98	1
	900	0.0622	2.78	1	1.34	1	3.36	1
SGS	144	0.0280	7.77	0.70	5.73	1.05	7.52	0.57
	361	0.0177	4.15	0.75	3.84	1.38	3.72	0.53
	900	0.0111	2.49	0.89	1.89	1.41	1.85	0.55
GRTS	144	0.1090	14.25	1.29	6.99	1.28	15.12	1.14
	361	0.1064	7.60	1.37	3.58	1.28	8.05	1.15
	900	0.1035	3.82	1.37	1.83	1.26	4.23	1.26
BAS	144	0.0524	9.52	0.86	4.90	0.90	9.82	0.74
	361	0.0631	5.29	0.95	2.82	1.01	6.27	0.90
	900	0.0564	3.05	1.10	1.33	0.99	3.08	0.92
HIP	144	0.0524	9.54	0.86	4.85	0.89	9.94	0.75
	361	0.0634	5.32	0.96	2.79	1.00	6.32	0.91
	900	0.0565	3.06	1.10	1.30	0.97	3.05	0.91

TABLE 4 Mean values of B, percentage ERSE and efficiencies of the HT estimator of the coverage of the last two categories with respect to TSS.

			Category 4		Category 5	
Scheme	***n***	$\overline{B}$	**ERSE (%)**	**Eff**	**ERSE (%)**	**Eff**
TSS	144	0.0641	27.13	1	3.07	1
	361	0.0630	15.23	1	1.55	1
	900	0.0622	7.65	1	0.75	1
SGS	144	0.0280	21.21	0.78	4.05	1.32
	361	0.0177	8.12	0.53	2.51	1.62
	900	0.0111	4.63	0.61	1.44	1.93
GRTS	144	0.1090	28.66	1.06	3.90	1.27
	361	0.1064	16.11	1.06	2.04	1.32
	900	0.1035	8.96	1.17	1.05	1.40
BAS	144	0.0524	25.28	0.93	2.51	0.82
	361	0.0631	15.92	1.05	1.35	0.88
	900	0.0564	7.19	0.94	0.66	0.89
HIP	144	0.0524	25.45	0.94	2.52	0.82
	361	0.0634	15.88	1.04	1.37	0.89
	900	0.0565	7.23	0.95	0.67	0.90

TABLE 5 Mean values of B, percentage ERSE and efficiencies of the HT estimator of the total of the interest variable with respect to TSS for the continuous surface.

Scheme	n	$\overline{B}$	ERSE (%)	Eff
TSS	144	0.0641	0.49	1
	361	0.0630	0.20	1
	900	0.0622	0.08	1
SGS	144	0.0280	4.13	8.43
	361	0.0177	2.62	13.40
	900	0.0111	1.65	20.94
GRTS	144	0.1090	1.19	2.44
	361	0.1064	0.62	3.17
	900	0.1035	0.32	4.04
BAS	144	0.0524	0.37	0.75
	361	0.0631	0.26	1.31
	900	0.0564	0.08	0.98
HIP	144	0.0524	0.34	0.69
	361	0.0634	0.24	1.21
	900	0.0565	0.06	0.82

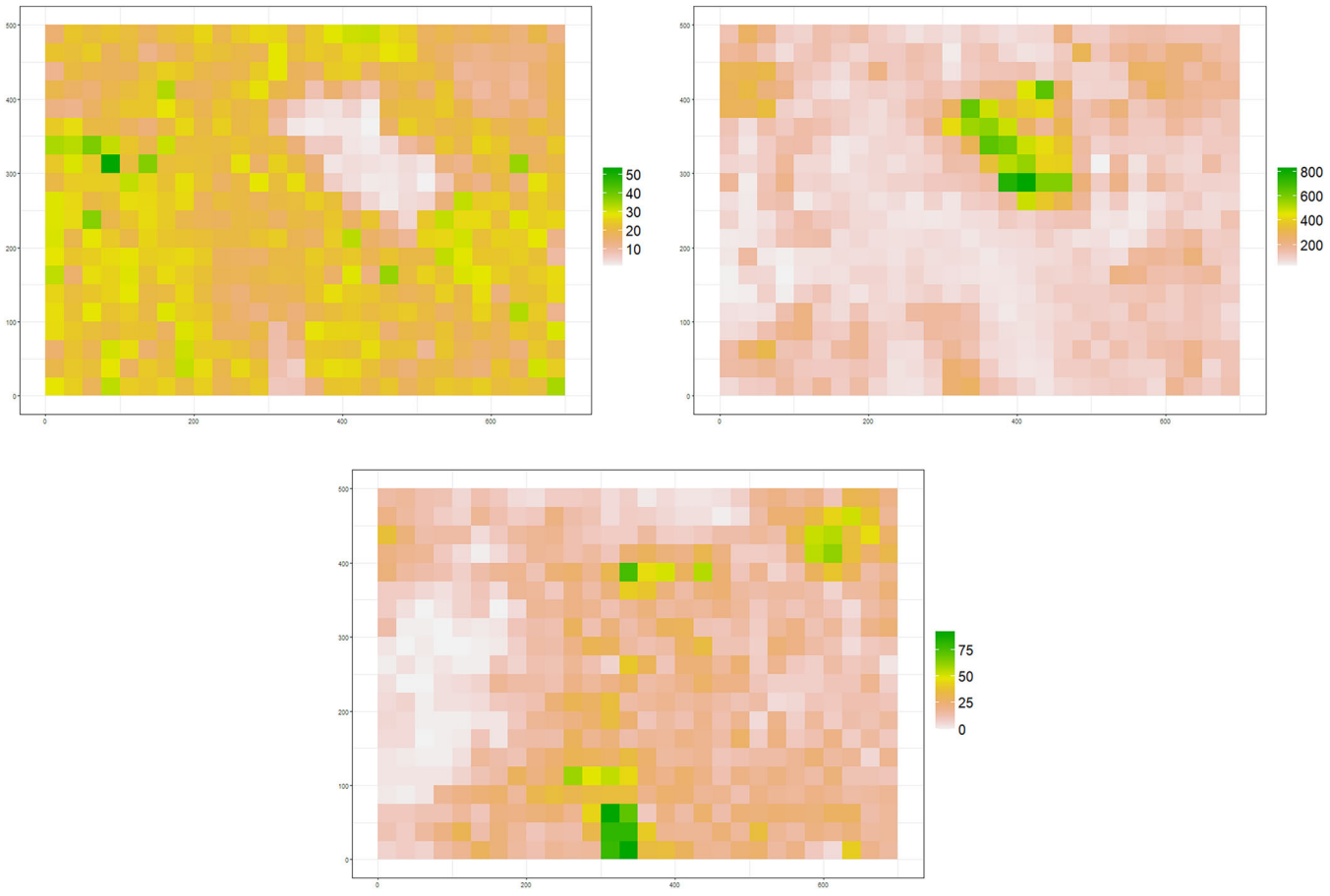

FIGURE 4 Population of 560 quadrats of 25-m side. Each quadrat is colored according to the total aboveground biomass (top left), the number of trees (top right) and the red maple abundance (bottom).

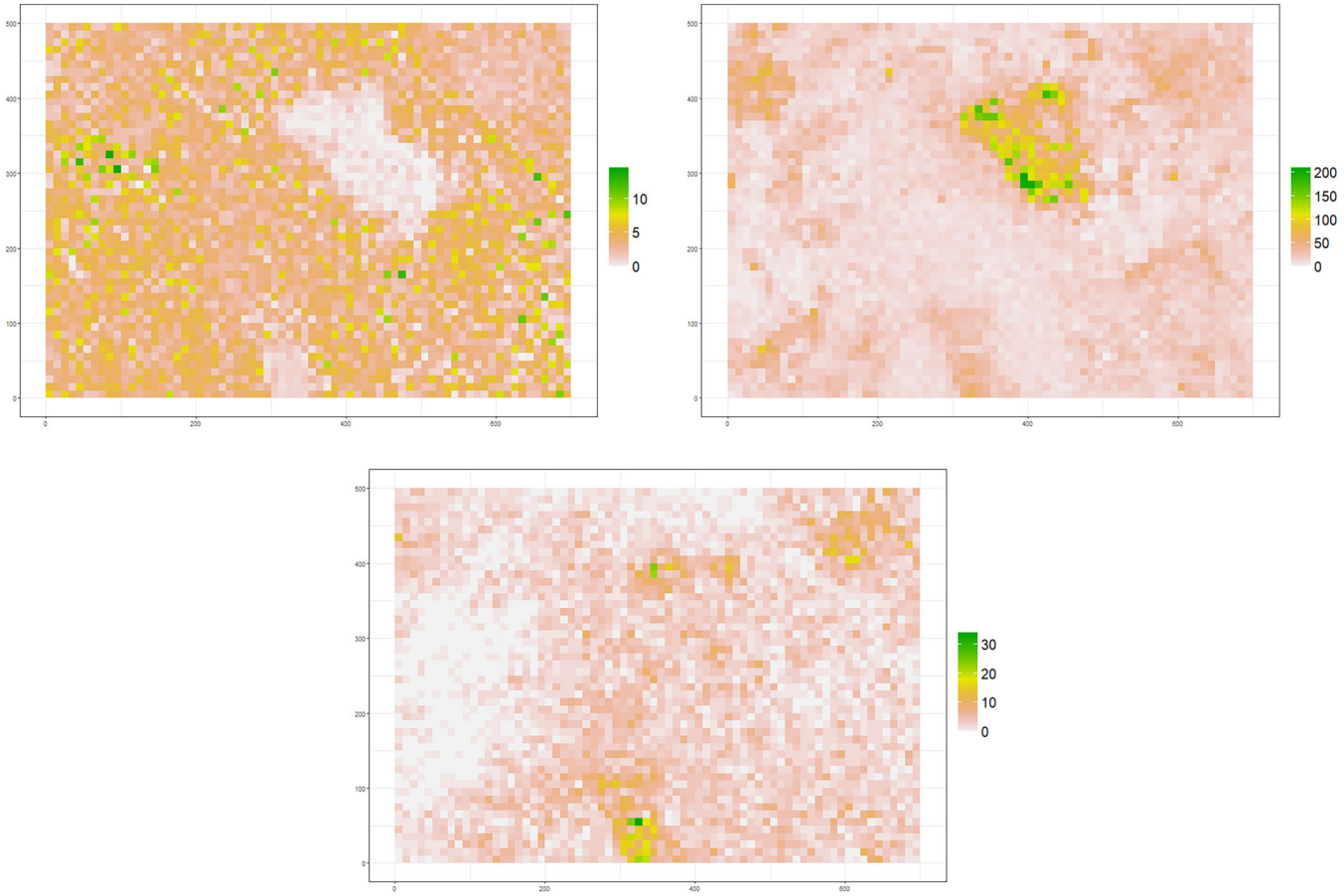

FIGURE 5 Population of 3500 quadrats of 10-m side. Each quadrat is colored according to the total aboveground biomass (top left), the number of trees (top right) and the red maple abundance (bottom).

is well known that SYS performance greatly depends on the population characteristics and large losses of precision with respect to SRSWOR may occur when spatial periodicities are present. OPSS and SYS satisfy the asymptotic spatial balance definition given by Fattorini, Marcheselli, and Pratelli (2018). Practically speaking, if the study region is partitioned into an increasing number of areas, these schemes are able to evenly spread sampled areas in such a way that any area is likely to have neighboring areas sampled. Fattorini, Marcheselli, and Pratelli (2018) also proved that under few mild regularity conditions, the two schemes guarantee the design-based consistency of the map of the density of the interest attribute obtained by using the inverse distance weighting interpolator.

If the population of areas arises from partitioning a study region where a fixed density function is defined, under the previous asymptotic setting, the HT estimator is proven to be design-based consistent under OPSS and under SYS (Fattorini et al., 2020, section 4.2). Alternatively, if a population of units is located in the study region, to prove consistency of the HT estimator under OPSS, it is also necessary to consider a sequence of nested populations of units of increasing size located in the study region and to suppose a sort of evenness in the enlargements of the nested populations in such a way that population units do not aggregate into some areas. In this case, consistency under SYS cannot be proven (Fattorini et al., 2020).

6 | SIMULATION STUDY

To compare the performances of the specifically tailored spatially balanced sampling schemes reviewed in Section 4 with those of the tessellation sampling schemes, an extensive simulation study is conducted on real and simulated populations. The main goal is to check whether, under constant first-order inclusion probabilities or inclusion density functions, more complex schemes allow for a valuable increase in precision with respect to tessellation schemes.

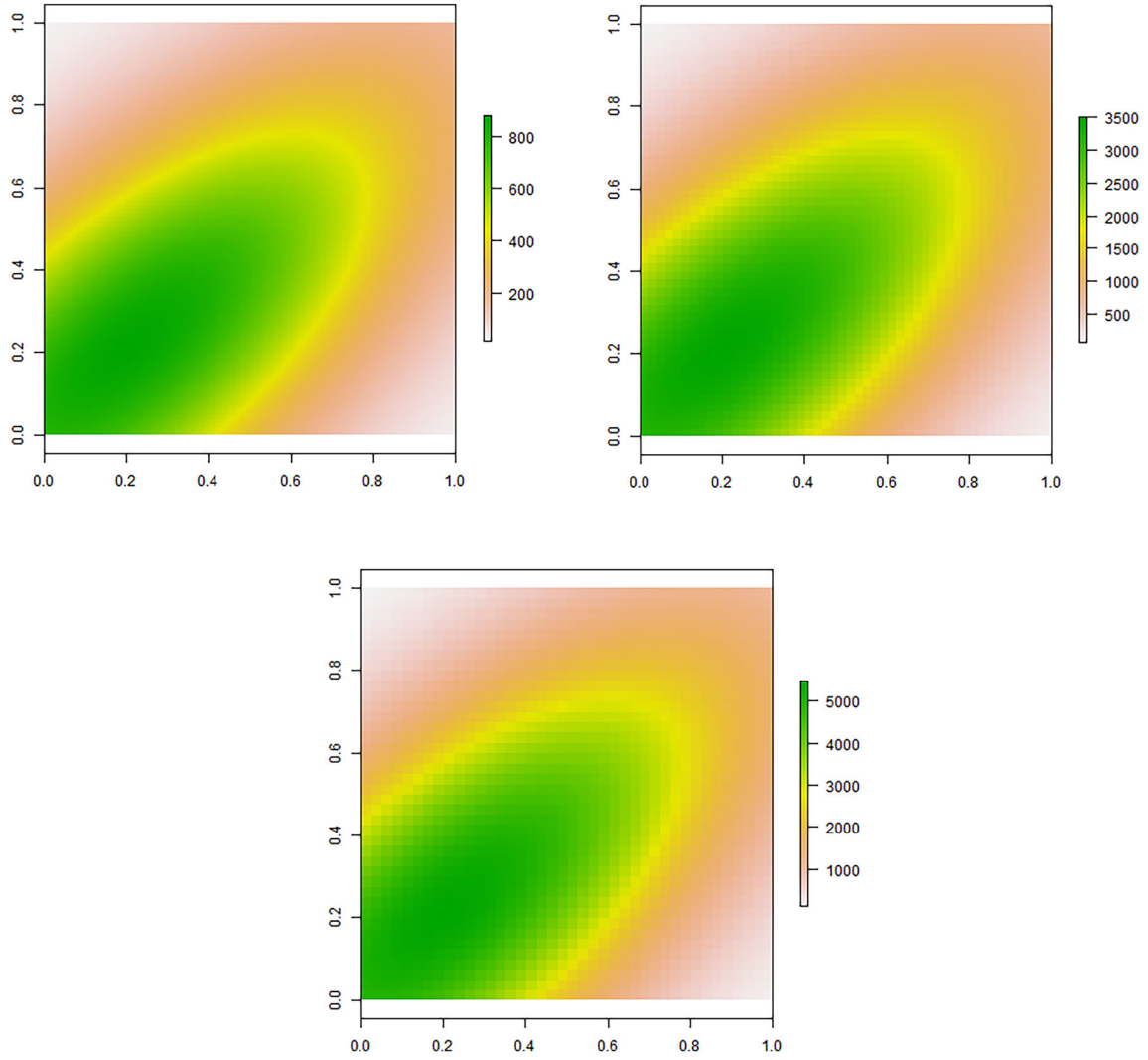

FIGURE 6 Populations of 1600 (top left), 2500 (top right), and 10,000 (bottom) quadrats obtained using the first artificial surface.

6.1 | Continuous populations

A real continuous population and two simulated continuous populations are considered. The real population is a $10 \times 10\,\text{km}^2$ region located between the provinces of Siena and Grosseto in southern Tuscany (central Italy), whose land use map was estimated (Marcelli et al., 2023) via a sample survey based on TSS during the "Inventario dell'Uso delle Terre d'Italia" (IUTI) project. In particular, the land use map (Figure 1) shows the 5 land use classes of forestland, cropland, grassland, wetland and settlements, whose coverages constitute the parameters to be estimated. The coverage T_j of the jth land use ($j = 1, \ldots, 5$) can be expressed as a total since, denoted by $\mathcal{A}_j$, the surface of the region covered by the jth land use ($j = 1, \ldots, 5$),

$$T_j = \int_{\mathcal{A}} I_{\mathcal{A}_j}(\mathbf{p})\lambda(d\mathbf{p}),$$

where $I_{\mathcal{A}_j}$ denotes the indicator function of $\mathcal{A}_j$.

To obtain the surface values $I_{\mathcal{A}_j}(\mathbf{p})$ for any location p, the estimated map was digitalized and converted to a shapefile using QGIS software (QGIS Development Team, 2023), resulting in coverages $70.46, 25.84, 2.63, 0.43, 0.64\ \text{km}^2$ for forestland, cropland, grassland, wetland, and settlements.

Sampling was performed by selecting $n = 144{,}361{,}900$ locations using TSS, SGS, GRTS, BAS, and HIP. TSS and SGS are implemented by partitioning the region into grids of 12×12, 19×19 and 30×30 quadrats. For the more complex

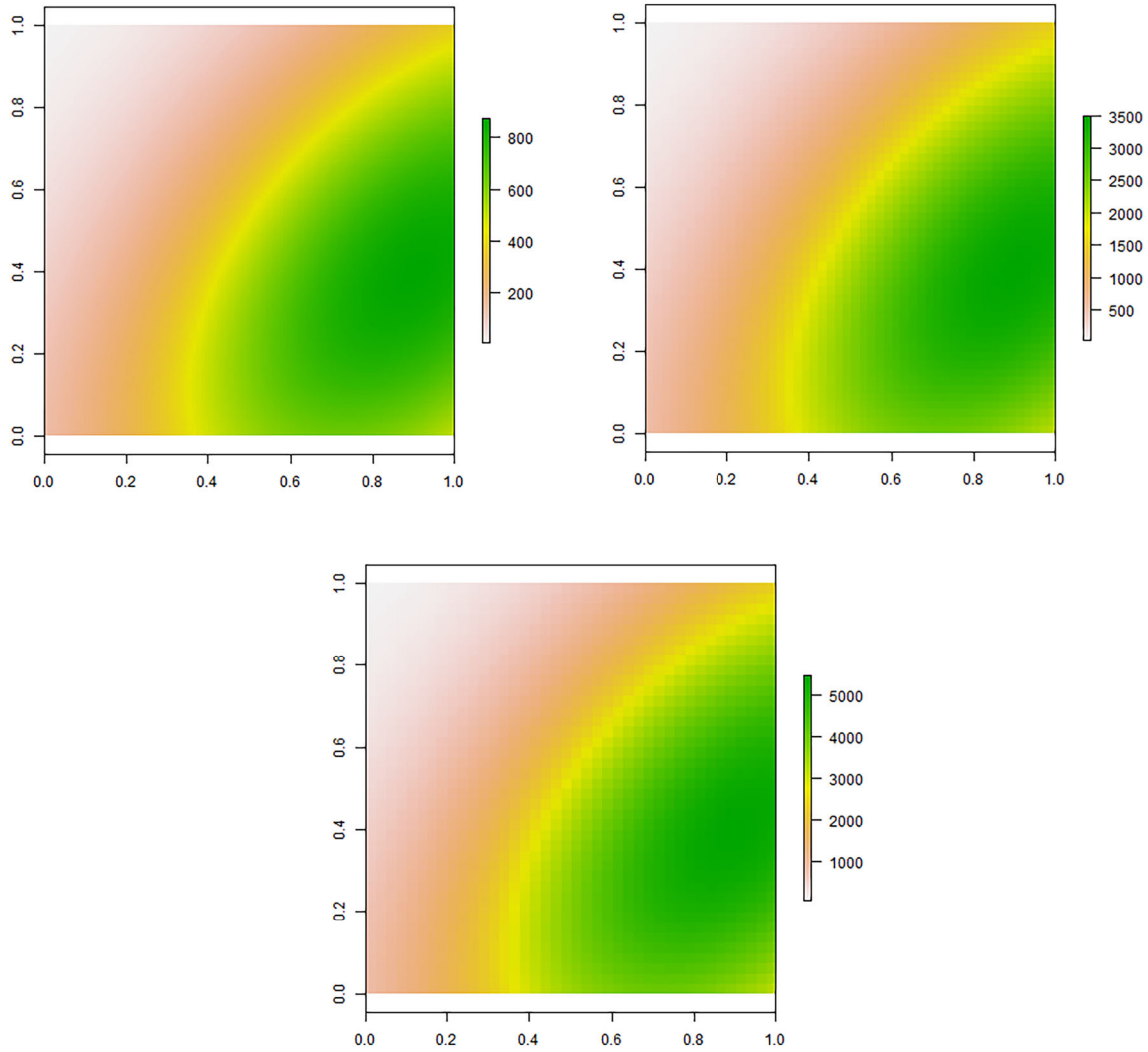

FIGURE 7 Populations of 1600 (top left), 2500 (top right), and 10,000 (bottom) quadrats obtained using the second artificial surface.

schemes, GRTS is performed by using the R (R Core Team, 2023) package "spsurvey" (Dumelle et al., 2023), and BAS and HIP are performed using the R package "SDraw" (McDonald & McDonald, 2020). However, the package "SDraw" has been removed from the CRAN repository (https://CRAN.R-project.org/package=SDraw), and has been installed from GitHub.

For each combination of sampling scheme $\mathcal{S}$ and sample size n, $R = 10{,}000$ samples are independently selected, and the coverage of each land use class j is estimated according to the HT estimator (2) as the ratio of the number of points in a given class to the total number of points multiplied by the size of the study region. From the Monte Carlo distributions of the HT estimates, the empirical standard error

$$\mathrm{ESE}_{\mathcal{S},j} = \sqrt{\frac{1}{R}\sum_{r=1}^{R}(\hat{T}_{\mathcal{S},rj} - T_j)^2}$$

is computed for each land use, where $\hat{T}_{\mathcal{S},rj}$ is the estimate achieved in the rth sample ($r = 1, \ldots, 10{,}000$) selected using the sampling scheme $\mathcal{S}$. Moreover, the empirical relative standard error $\mathrm{ERSE}_{\mathcal{S},j} = \mathrm{ESE}_{\mathcal{S},j}/T_j$ is also obtained, and for each land use j, the performance of the scheme $\mathcal{S}$ is compared to that of TSS by computing the efficiency

$$\mathrm{Eff}_{\mathcal{S},j} = \frac{\mathrm{ESE}_{\mathcal{S},j}}{\mathrm{ESE}_{TSS,j}}.$$

TABLE 6 Mean values of B, percentage ERSE and efficiencies, with respect to OPSS, of the HT estimator of the total of the interest variables for the finite population of 560 quadrats obtained from partitioning the Harvard Forest study region.

			T_{AGB}		T_{trees}		T_{acer}	
Scheme	f	$\overline{B}$	**ERSE (%)**	**Eff**	**ERSE (%)**	**Eff**	**ERSE (%)**	**Eff**
OPSS	3.6%	0.0722	5.87	1	13.77	1	12.76	1
	10%	0.0741	3.09	1	6.73	1	6.10	1
	25%	0.0450	1.52	1	3.18	1	2.98	1
SYS	3.6%	0.0733	5.09	0.87	11.20	0.81	11.52	0.90
	10%	0.0495	2.95	0.95	6.21	0.92	9.11	1.49
	25%	0.0215	0.78	0.52	1.67	0.52	2.78	0.93
LPM	3.6%	0.0741	5.87	1.00	12.85	0.93	12.43	0.97
	10%	0.0619	3.04	0.98	6.16	0.92	6.13	1.01
	25%	0.0601	1.65	1.08	3.21	1.01	3.23	1.08
GRTS	3.6%	0.1186	5.95	1.01	13.77	1.00	13.62	1.07
	10%	0.1077	3.21	1.04	7.25	1.08	6.84	1.12
	25%	0.0944	1.76	1.16	3.86	1.21	3.59	1.20
SCPS	3.6%	0.0583	5.68	0.97	12.35	0.90	12.10	0.95
	10%	0.0472	2.95	0.95	5.98	0.89	5.81	0.95
	25%	0.0453	1.57	1.03	2.97	0.93	2.96	0.99
BAS	3.6%	0.1415	5.80	0.99	13.09	0.95	12.57	0.98
	10%	0.1421	3.08	1.00	7.01	1.04	7.09	1.16
	25%	0.1322	1.87	1.23	4.15	1.30	4.08	1.37
DBSS1	3.6%	0.0652	5.70	0.97	12.43	0.90	12.37	0.97
	10%	0.0533	2.92	0.95	6.05	0.90	6.19	1.01
	25%	0.0485	1.57	1.03	2.96	0.93	3.07	1.03
DBSS2	3.6%	0.0686	5.84	0.99	12.70	0.92	12.42	0.97
	10%	0.0546	2.97	0.96	6.10	0.91	6.02	0.99
	25%	0.0497	1.54	1.01	2.95	0.93	3.04	1.02

To quantify the degree of spatial balance of the samples selected under S, (5) is computed for each sample, and the average $\overline{B}$, the percentage values of the ERSEs and the values of the efficiencies for forestland, cropland and grassland are reported in Table 1. In all the tables, the efficiency is simply indicated as Eff to avoid unnecessarily burdening the notation. Table 2 reports the analogous values for wetland and settlements, which are the classes with coverage smaller than 1 km^2.

The simulation results in Tables 1 and 2 highlight the superiority of SGS, with only a few exceptions when considering the estimation of settlements coverage with the smallest sample size (Table 2). The performance of TSS is lightly better than that of GRTS and comparable to those of BAS and HIP, with efficiencies fluctuating between 0.86 and 1.24 with respect to BAS and HIP and many values quite close to 1. Notably, the lowest values of $\overline{B}$ are obtained under SGS. However, in the remaining cases, the lowest values of $\overline{B}$ do not necessarily correspond to the schemes that achieve better performances in terms of precision.

To consider different types of populations and trends, two artificial continuous populations in the unit square region are also considered, with the surface values defined at any location by the densities of the bivariate normal distributions with the following parameters: $\mu_1 = 0.2, \sigma_1^2 = 0.5, \mu_2 = 0.21, \sigma_2^2 = 0.45, \rho = 0.7$ and $\mu_1 = 0.9, \sigma_1^2 = 0.47, \mu_2 = 0.4, \sigma_2^2 = 0.5, \rho = 0.5$.

In the first case, the surface values were grouped into 5 classes to obtain a land use map with a notably different distribution of land use categories compared to the IUTI map (see Figure 2). In particular, surface values smaller than

TABLE 7 Mean values of B, percentage ERSE and efficiencies of the HT estimator of the total of the interest variables for the finite population of 3500 quadrats obtained from partitioning the Harvard Forest study region.

			T_{AGB}		T_{trees}		T_{acer}	
Scheme	f	$\overline{B}$	**ERSE (%)**	**Eff**	**ERSE (%)**	**Eff**	**ERSE (%)**	**Eff**
OPSS	4%	0.0611	4.21	1	5.16	1	6.12	1
	10%	0.0697	2.57	1	2.85	1	3.57	1
	25%	0.0439	1.48	1	1.41	1	1.97	1
SYS	4%	0.0275	4.22	1.00	4.20	0.81	5.62	0.92
	10%	0.0166	2.23	0.87	1.32	0.47	3.51	0.98
	25%	0.0086	1.73	1.17	0.94	0.66	0.89	0.45
LPM	4%	0.0573	4.23	1.00	4.93	0.95	6.18	1.01
	10%	0.0534	2.57	1.00	2.75	0.97	3.54	0.99
	25%	0.0564	1.52	1.02	1.48	1.05	1.99	1.01
GRTS	4%	0.1093	4.30	1.02	5.53	1.07	6.54	1.07
	10%	0.1040	2.64	1.03	3.08	1.08	3.83	1.07
	25%	0.0906	1.51	1.02	1.60	1.13	2.15	1.09
SCPS	4%	0.0413	4.21	1.00	4.79	0.93	6.08	0.99
	10%	0.0383	2.59	1.01	2.67	0.94	3.50	0.98
	25%	0.0406	1.52	1.03	1.41	1.00	1.96	1.00
BAS	4%	0.1464	4.34	1.03	5.93	1.15	6.55	1.07
	10%	0.1359	2.62	1.02	3.80	1.33	3.58	1.00
	25%	0.1436	1.49	1.01	2.14	1.52	2.06	1.05
DBSS1	4%	0.0490	4.19	0.99	4.86	0.94	6.12	1.00
	10%	0.0450	2.61	1.02	2.68	0.94	3.59	1.00
	25%	0.0446	1.51	1.02	1.42	1.01	1.96	0.99
DBSS2	4%	0.0487	4.27	1.01	4.79	0.93	6.10	1.00
	10%	0.0443	2.58	1.00	2.65	0.93	3.50	0.98
	25%	0.0458	1.51	1.02	1.40	1.00	1.97	1.00

1 were assigned to the first category, values greater than or equal to 1 and smaller than 3 were assigned to the second category, values greater than or equal to 3 and smaller than 4 were assigned to the third category, values greater than or equal to 4 and smaller than 4.5 were assigned to the fourth category and values greater than 4.5 were assigned to the last category. The coverage of category 1 is 0.08, that of category 2 is 0.30, that of category 3 is 0.14, that of category 4 is 0.06 and that of category 5 is 0.42. Additionally, in this case, the parameters of interest are the coverages of the five categories and are estimated as in the case of the real continuous population. In the second scenario, the surface values (Figure 3) represent the density of an attribute of interest, and the parameter is a total of type (1), which is estimated by means of (2).

For both artificial populations, the simulation is implemented as in the real population case. Indeed, $R = 10{,}000$ samples of size $n = 144{,}361, 900$ are selected according to TSS, SGS, GRTS, BAS, and HIP and the ERSEs, the efficiencies with respect to TSS and the averages of the B values are reported in Tables 3 and 4 for the land use map and in Table 5 for the continuous surface.

According to the results in Tables 3 and 4, when estimating coverages, SGS achieves the best performance in terms of precision for categories 1, 3 (see Table 3) and 4 (see Table 4), while TSS yields lower ERSE values for the remaining two categories. Moreover, TSS outperforms GRTS, sometimes achieving remarkable gains in precision. For BAS and HIP, their efficiencies range between 0.74 and 1.04, with smaller values achieved for the smallest sample sizes. The lowest values of $\overline{B}$ are achieved under SGS, which does not always yield the highest precision (see results for category 2 in Table 3 and category 5 in Table 4).

TABLE 8 Mean values of B, percentage ERSE and efficiencies of the HT estimator of the total of the interest variable for the two simulated populations partitioned into 1600 quadrats.

			Surface 1		Surface 2	
Scheme	***n***	$\overline{B}$	**ERSE (%)**	**Eff**	**ERSE (%)**	**Eff**
OPSS	4%	0.0629	1 .29	1	1 .09	1
	10%	0.0719	0.58	1	0.55	1
	25%	0.0454	0.18	1	0.15	1
SYS	4%	0.0404	3.01	2.34	6.05	5.57
	10%	0.0265	2.14	3.68	5.52	10.05
	25%	0.0141	1.05	5.68	2.14	14.03
LPM	4%	0.0617	1.63	1.27	1.47	1.35
	10%	0.0563	0.68	1.18	0.62	1.13
	25%	0.0580	0.29	1.56	0.25	1.67
GRTS	4%	0.0630	1.29	1.00	1.08	0.99
	10%	0.0971	0.86	1.48	0.72	1.31
	25%	0.0922	0.41	2.22	0.34	2.21
SCPS	4%	0.0459	1.33	1.04	0.93	0.86
	10%	0.0413	0.50	0.86	0.38	0.70
	25%	0.0425	0.19	1.05	0.16	1.03
BAS	4%	0.2579	10.33	8.03	4.93	4.54
	10%	0.1526	5.01	8.60	2.41	4.40
	25%	0.1152	1.99	10.74	1.29	8.43
DBSS1	4%	0.0535	1.26	0.98	1.01	0.93
	10%	0.0479	0.51	0.88	0.41	0.75
	25%	0.0463	0.20	1.09	0.16	1.08
DBSS2	4%	0.0540	1.32	1.03	1.02	0.94
	10%	0.0477	0.53	0.91	0.41	0.76
	25%	0.0476	0.21	1.14	0.16	1.07

For the artificial continuous population, the results in Table 5 show that the lowest values of $\overline{B}$ are associated with the worst performance in terms of precision, with the ERSE values under SGS being remarkably larger than those achieved under TSS. Additionally, in this case, the TSS performances are superior to those of the GRTS and comparable to those of the HIP and BAS.

6.2 | Finite population of areas

Several finite populations of areas are obtained based on the Harvard Forest community of trees (Orwig et al., 2023) in Massachusetts (USA), while to consider different spatial trends, other finite populations are derived from two artificial surfaces.

The Harvard Forest community is a 35 ha rectangular portion (500 m × 700 m) of temperate forest, and consequently, the dominant species include white pine (Pinus strobus), red oak (Quercus rubra), red maple (Acer rubrum) and eastern hemlock (Tsuga canadensis). The first census was conducted from 2010 to 2014. During the summers of 2010 and 2011, all woody stems with a diameter at breast height of at least 1 cm were enumerated, and their spatial coordinates were recorded, while the dense shrubs in the swamp section located in the center of the area were censused when frozen during the winters of 2012–2014. In particular, $T_{\text{trees}} = 77{,}536$ living trees partitioned into 55 species were censused.

TABLE 9 Mean values of B, percentage ERSE and efficiencies of the HT estimator of the total of the interest variable for the two simulated populations partitioned into 2500 quadrats.

			Surface 1		Surface 2	
Scheme	n	$\overline{B}$	**ERSE (%)**	**Eff**	**ERSE (%)**	**Eff**
OPSS	4%	0.0620	0.82	1	0.69	1
	10%	0.0712	0.38	1	0.35	1
	25%	0.0442	0.12	1	0.10	1
SYS	4%	0.0319	2.37	2.88	4.84	6.98
	10%	0.0209	1.69	4.45	4.38	12.46
	25%	0.0151	0.84	7.02	1.72	17.57
LPM	4%	0.0591	1.07	1.30	0.97	1.40
	10%	0.0548	0.45	1.19	0.41	1.17
	25%	0.0576	0.19	1.57	0.17	1.70
GRTS	4%	0.1098	1.51	1.83	1.28	1.84
	10%	0.1035	0.71	1.87	0.64	1.83
	25%	0.0913	0.31	2.56	0.28	2.82
SCPS	4%	0.0429	0.85	1.03	0.60	0.86
	10%	0.0397	0.31	0.82	0.24	0.68
	25%	0.0421	0.12	1.05	0.10	1.01
BAS	4%	0.1428	3.04	3.69	3.13	4.52
	10%	0.1296	1.73	4.56	2.12	6.01
	25%	0.1296	1.13	9.44	1.51	15.44
DBSS1	4%	0.0506	0.81	0.98	0.66	0.95
	10%	0.0464	0.33	0.86	0.26	0.75
	25%	0.0462	0.13	1.10	0.10	1.07
DBSS2	4%	0.0506	0.87	1.05	0.66	0.95
	10%	0.0458	0.34	0.90	0.26	0.75
	25%	0.0472	0.14	1.14	0.11	1.08

Two finite populations of areas are obtained by considering two different partitions of the region: the first population is composed of $N = 560$ quadrats of 25-m side, and the second population is composed of $N = 3500$ quadrats of 10-m side. For each quadrat of each population, the total aboveground biomass was computed as the sum of the aboveground biomass of the trees within the quadrat, and similarly, the total number of trees and the red maple abundance were counted. Figures 4 and 5 show maps of the total aboveground biomass, the total abundance and the red maple abundance for the first population and second population, respectively.

Sampling is performed by means of OPSS, SYS, LPM, GRTS, SCPS, BAS, and DBSS, all with equal first-order inclusion probabilities. In the first population, increasing sampling fractions of 3.6%, 10%, and 25%, corresponding to sample sizes of $n = 20, 56, 140$, are considered, while in the second population, sampling fractions of 4%, 10%, and 25%, corresponding to sample sizes of $n = 140, 350, 875$, are considered. To implement OPSS and SYS in the first population, quadrats are grouped into strata/blocks of 7×4, 2×5, and 2×2 quadrats, while in the second population, they are grouped into strata/blocks of 5×5, 5×2, and 2×2 quadrats.

The R package "BalancedSampling" (Grafström et al., 2022) was used to select samples by means of LPM, SCPS, and DBSS. In particular, LPM of type 1 (Grafström et al., 2012) and SCPS with maximal weights (Grafström, 2012) are performed. For DBSS, balance is obtained using both inclusion probabilities and spatial coordinates (DBSS1) and inclusion probabilities, spatial coordinates and their squared values (DBSS2). Additionally, in this case, GRTS is implemented by

TABLE 10 Mean values of B, percentage ERSE and efficiencies of the HT estimator of the total of the interest variable for the two simulated populations partitioned into 10,000 quadrats.

			Surface 1		Surface 2	
Scheme	***n***	$\overline{B}$	**ERSE (%)**	**Eff**	**ERSE (%)**	**Eff**
OPSS	4%	0.0601	0.21	1	0.17	1
	10%	0.0687	0.10	1	0.09	1
	25%	0.0440	0.03	1	0.02	1
SYS	4%	0.0161	1.18	5.65	2.45	14.07
	10%	0.0105	0.84	8.76	2.20	24.56
	25%	0.0056	0.42	14.07	0.86	34.82
LPM	4%	0.0535	0.29	1.40	0.26	1.48
	10%	0.0512	0.12	1.26	0.11	1.21
	25%	0.0555	0.05	1.72	0.04	1.80
GRTS	4%	0.1047	0.40	1.92	0.33	1.90
	10%	0.0999	0.19	2.00	0.16	1.83
	25%	0.0885	0.08	2.81	0.07	2.87
SCPS	4%	0.0372	0.19	0.93	0.14	0.83
	10%	0.0358	0.08	0.78	0.06	0.65
	25%	0.0394	0.03	1.04	0.02	1.00
BAS	4%	0.1326	1.30	6.24	1.22	7.04
	10%	0.1393	0.82	8.52	0.75	8.38
	25%	0.1361	0.39	13.15	0.38	15.42
DBSS1	4%	0.0450	0.20	0.98	0.17	0.95
	10%	0.0427	0.08	0.85	0.07	0.73
	25%	0.0437	0.03	1.10	0.03	1.06
DBSS2	4%	0.0440	0.22	1.04	0.16	0.95
	10%	0.0415	0.09	0.90	0.07	0.74
	25%	0.0448	0.03	1.15	0.03	1.08

means of the "spsurvey" package (Dumelle et al., 2023), and the "SDraw" package (McDonald & McDonald, 2020) is adopted for BAS. Notably, HIP is not implemented because "SDraw" did not run properly with these populations.

For each combination of population, sampling scheme and sampling fraction, $R = 10{,}000$ samples are independently selected, and the population total aboveground biomass T_{AGB}, the population total number of trees T_{trees} and the population red maple abundance T_{acer} are estimated by means of (4). Then, the ERSE values are computed from the Monte Carlo distributions of the estimates, and in this case, the efficiencies of the more complex schemes are computed with respect to OPSS and obtained as the ratio of the corresponding empirical standard errors, with those of OPSS at the denominator.

The surfaces adopted to construct the artificial populations of areas are those already considered in the continuous population setting. To construct three finite populations, the unit square is partitioned into $N = 40 \times 40$, $N = 50 \times 50$, and $N = 100 \times 100$ quadrats, and the total amount of the attribute of interest in each quadrat is obtained by using the R package "raster" (Hijmans, 2023) and, in particular, its function "aggregate." Figures 6 and 7 depict the populations of quadrats when the first surface and second surface are considered, respectively. Additionally, in this case, sampling is performed by means of OPSS, SYS, LPM, GRTS, SCPS, BAS, and DBSS, all with equal first-order inclusion probabilities, using the packages "spsurvey" (Dumelle et al., 2023) and "SDraw" (McDonald & McDonald, 2020). DBSS is implemented as in the real finite population case, and to perform OPSS and SYS, quadrats are grouped into strata/blocks of 5×5, 2×5 and 2×2. Increasing sampling fractions of 4%, 10%, and 25% are considered for each population size N, which corresponds

to a sample size of $n = 64,160,400$, $n = 100,250,625$, and $n = 400,1000,2500$, respectively. For each combination of population, sampling scheme and sampling fraction, $R = 10,000$ samples are independently selected, and by means of the Monte Carlo estimate distributions, the ERSE values and efficiencies with respect to OPSS are computed and reported in Tables 8–10.

The simulation results in Tables 6–10 confirm the well-known characteristics of the SYS: there are cases where it can work very well but also cases where it shows dramatically poor performance. OPSS outperforms GRTS and, generally, BAS. The performances of OPSS, LPM, and DBSS are very similar for real populations (see Tables 6 and 7), while for artificial populations (see Tables 8–10), OPSS is superior to LPM, while the efficiencies of DBSS are variable, ranging from 0.73 to 1.15. The performances of OPSS and SCPS are very similar for real populations, while for artificial populations, SCPS can sometimes achieve better precision. In this case, better precisions do not necessarily correspond to lower values of $\overline{B}$, as evidenced by the results in Tables 8–10, in which SYS achieves the lowest values of $\overline{B}$ and the worst efficiencies.

7 | CONCLUDING REMARKS

Many schemes for achieving spatial balance have been proposed in the literature. R packages are available only for some of them, thus rendering their implementation less complex, even though it may be difficult, especially for practitioners, to understand the sample selection process.

Not surprisingly, the simulation results show that none of the considered schemes performs markedly better than the others for any combination of population, sample size or parameter of interest under constant first-order inclusion probabilities or inclusion density functions. However, regarding the finite sample performance of the tessellation schemes, SGS and SYS can achieve very high precision but sometimes yield poor performance, while the performances of TSS and OPSS are generally comparable to, and sometimes better than, those of the specifically tailored spatially balanced schemes. Moreover, the simulation results show that the lower values of the spatial balance measure by Stevens and Olsen (2004), achieved under SGS and SYS, do not necessarily correspond to greater precision.

The asymptotic properties of the HT estimator (Fattorini et al., 2020) and of the estimated map of the density of the attribute of interest (Fattorini, Marcheselli, Pisani, & Pratelli, 2018; Fattorini, Marcheselli, & Pratelli, 2018), which are guaranteed by the tessellation schemes under suitable conditions, cannot be proven to hold for the specifically tailored schemes, owing to their complexity. However, their effectiveness in providing spatial balance may lead to the presumption that these properties also hold for these schemes. The use of TSS and OPSS for achieving spatial balance and improving precision is supported by the simulation results, their asymptotic properties and the simplicity of the sampling selection procedure, which, as noted by Tillé and Wilhelm (2017), is among the important aspects when choosing the sampling design.

Complex schemes allow the use of additional auxiliary information to spread the sample in the auxiliary variable space and/or to calibrate first-order inclusion probabilities, even if the complexity of their implementation obviously increases. However, when the sample is spread in the auxiliary variable space, balance in the geographic space may be lost, while there are situations such as national forest inventories, where it is an essential requirement. An alternative approach to exploiting additional auxiliary information could be the use of model-assisted estimators and tessellation sampling schemes, and further research should be devoted to evaluating the efficiency of these strategies.

ACKNOWLEDGMENTS

The authors thank Lorenzo Fattorini from the University of Siena for stimulating this research and providing many suggestions. Open access publishing facilitated by Universita degli Studi di Siena, as part of the Wiley - CRUI-CARE agreement.

FUNDING INFORMATION

Project funded under the National Recovery and Resilience Plan (NRRP), Mission 4 Component 2 Investment 1.4–Call for tender No. 3138 of 16 December 2021, rectified by Decree n.3175 of 18 December 2021 of Italian Ministry of University and Research funded by the European Union—NextGenerationEU; Award Number: Project code CN_00000033, Concession Decree No. 1034 of 17 June 2022 adopted by the Italian Ministry of University and Research, CUP B63C22000650007, Project title "National Biodiversity Future Center–NBFC."

DATA AVAILABILITY STATEMENT

The data that support the findings of this study are available on request from the corresponding author. The data are not publicly available due to privacy or ethical restrictions.

REFERENCES

Barabesi, L., Franceschi, S., & Marcheselli, M. (2012). Properties of design-based estimation under stratified spatial sampling with application to canopy coverage estimation. *Annals of Applied Statistics*, *6*, 210–228.

Benedetti, R., Piersimoni, F., & Postiglione, P. (2017). Spatially balanced sampling: a review and a reappraisal. *International Statistical Review*, *85*, 439–454.

Bondesson, L., & Thorburn, D. (2008). A list sequential sampling method suitable for real-time sampling. *Scandinavian Journal of Statistics*, *35*, 466–483.

Cordy, C. B. (1993). An extension of the Horvitz-Thompson theorem to point sampling from a continuous universe. *Statistics & Probability Letters*, *18*, 353–362.

Cressie, N. (1993). *Statistics for spatial data*. John Wiley.

Development Team, Q. G. I. S. (2023). *QGIS geographic information system*. Open Source Geospatial Foundation. http://qgis.org

Deville, J. C., & Tillé, Y. (1998). Unequal probability sampling without replacement through a splitting method. *Biometrika*, *85*, 89–101.

Deville, J. C., & Tillé, Y. (2004). Efficient balanced sampling: the cube method. *Biometrika*, *91*, 893–912.

Dumelle, M., Kincaid, T., Olsen, A. R., & Weber, M. (2023). spsurvey: Spatial sampling design and analysis in R. *Journal of Statistical Software*, *105*(3), 1–29.

Fattorini, L. (2006). Applying the Horvitz-Thompson criterion in complex designs: a computer-intensive perspective for estimating inclusion probabilities. *Biometrika*, *93*, 269–278.

Fattorini, L., Marcheselli, M., Pisani, C., & Pratelli, L. (2018). Design-based maps for continuous spatial populations. *Biometrika*, *105*, 419–429.

Fattorini, L., Marcheselli, M., Pisani, C., & Pratelli, L. (2020). Design-based consistency of the Horvitz-Thompson estimator under spatial sampling with applications to environmental surveys. *Spatial Statistics*, *35*, 100404.

Fattorini, L., Marcheselli, M., & Pratelli, L. (2018). Design-based maps for finite populations of spatial units. *Journal of the American Statistical Association*, *113*, 686–697.

Grafström, A. (2012). Spatially correlated Poisson sampling. *Journal of Statistical Planning and Inference*, *142*, 139–147.

Grafström, A., Lisic, J. and Prentius, W. (2022), *BalancedSampling: Balanced and spatially balanced sampling*. R package version 1.6.3. https://CRAN.R-project.org/package=BalancedSampling

Grafström, A., & Lundström, N. L. (2013). Why well spread probability samples are balanced. *Open Journal of Statistics*, *3*, 36–41.

Grafström, A., Lundström, N. L., & Schelin, L. (2012). Spatially balanced sampling through the pivotal method. *Biometrics*, *68*, 514–520.

Grafström, A., & Matei, A. (2018). Spatially balanced sampling of continuous populations. *Scandinavian Journal of Statistics*, *45*, 792–805.

Grafström, A., & Schelin, L. (2014). How to select representative samples. *Scandinavian Journal of Statistics*, *41*, 277–290.

Grafström, A., Schnell, S., Saarela, S., Hubbell, S., & Condit, R. (2017). The continuous population approach to forest inventories and use of information in the design. *Environmetrics*, *28*, e2480.

Grafström, A., & Tillé, Y. (2013). Doubly balanced spatial sampling with spreading and restitution of auxiliary totals. *Environmetrics*, *24*, 120–131.

Grafström, A., Zhao, X., Nylander, M., & Petersson, H. (2017). A new sampling strategy for forest inventories applied to the temporary clusters of the Swedish national forest inventory. *Canadian Journal of Forest Research*, *47*, 1161–1167.

Gregoire, T. G., & Valentine, H. T. (2007). *Sampling strategies for natural resources and the environment*. CRC Press.

Hedayat, A., & Sinha, B. K. (1991). *Design and inference in finite population sampling*. John Wiley.

Hijmans, R. J. (2023), *raster: Geographic data analysis and modeling*. R package version 3.6-20. https://CRAN.R-project.org/package=raster

Jauslin, R., & Tillé, Y. (2020). Spatial spread sampling using weakly associated vectors. *Journal of Agricultural, Biological and Environmental Statistics*, *25*, 431–451.

Jauslin, R. and Tillé, Y. (2022), *WaveSampling: Weakly associated vectors (WAVE) sampling*. R package version 0.1.3. https://CRAN.R-project.org/package=WaveSampling

Kermorvant, C., D'amico, F., Bru, N., Caill-Milly, N., & Robertson, B. (2019). Spatially balanced sampling designs for environmental surveys. *Environmental Monitoring and Assessment*, *191*, 524.

Mandallaz, D. (2007). *Sampling techniques for forest inventories*. CRC Press.

Marcelli, A., Di Biase, R. M., Corona, P., Stehman, S., & Fattorini, L. (2023). Design-based mapping of land use/land cover classes with bootstrap estimation of precision by nearest-neighbour interpolation. *Annals of Applied Statistics*, *17*, 3133–3152.

McDonald, T., & McDonald, A. (2020). SDraw: Spatially balanced samples of spatial objects. R package version 2.1.13 https://github.com/tmcd82070/SDraw/wiki/SDraw

Orwig, D., Foster, D. and Ellison, A. (2023), *Harvard forest CTFS-ForestGEO mapped forest plot since 2014*, Harvard Forest Data Archive: HF253 (v.6). Environmental Data Initiative. https://doi.org/10.6073/pasta/818789a882a318c1d7f3fc43a2289e12

R Core Team. (2023). *R: A language and environment for statistical computing*. R Foundation for Statistical Computing. https://www.R-project.org/

Robertson, B., Brown, J., McDonald, T., & Jaksons, P. (2013). BAS: Balanced acceptance sampling of natural resources. *Biometrics*, *69*, 776–784.

Robertson, B., McDonald, T., Price, C., & Brown, J. (2017). A modification of balanced acceptance sampling. *Statistics & Probability Letters*, *129*, 107–112.

Robertson, B., McDonald, T., Price, C., & Brown, J. (2018). Halton iterative partitioning: spatially balanced sampling via partitioning. *Environmental and Ecological Statistics*, *25*, 305–323.

Stevens, D. L. (1997). Variable density grid-based sampling designs for continuous spatial populations. *Environmetrics*, *8*, 167–195.

Stevens, D. L., & Olsen, A. R. (2003). Variance estimation for spatially balanced samples of environmental resources. *Environmetrics*, *14*, 593–610.

Stevens, D. L., & Olsen, A. R. (2004). Spatially balanced sampling of natural resources. *Journal of the American Statistical Association*, *99*, 262–278.

Stevens, D. L., & Urquhart, N. S. (2000). Response designs and support regions in sampling continuous domains. *Environmetrics*, *11*, 13–41.

Tillé, Y., Dickson, M. M., Espa, G., & Giuliani, D. (2018). Measuring the spatial balance of a sample: A new measure based on Moran's I index. *Spatial Statistics*, *23*, 182–192.

Tillé, Y., & Wilhelm, M. (2017). Probability sampling designs: principles for choice of design and balancing. *Statistical Science*, *32*, 176–189.

Tomppo, E., Gschwantner, T., Lawrence, M., & McRoberts, R. E. (Eds.). (2010). *National forest inventories*. Springer.

Wolter, K. M. (2007). *Introduction to variance estimation*. Springer.

How to cite this article: Di Biase, R. M., Marcheselli, M., & Pisani, C. (2025). Achieving spatial balance in environmental surveys under constant inclusion probabilities or inclusion density functions. *Environmetrics*, *36*(1), e2869. https://doi.org/10.1002/env.2869